18th International Conference on Ships and Shipping Research 2015, June 24th – 26th, Lecco, Italy

M. Altosole and A. Francescutto (Editors)

INFLUENCE OF SEA STATE MODELS ON CALCULATED NAVAL VESSEL STRESS SPECTRA

Ian THOMPSON

DRDC Atlantic Research Centre, Dartmouth, NS, Canada, ian.thompson@drdc-rddc.gc.ca

ABSTRACT

Fatigue damage is a governing factor in a naval ship's design life, can limit the vessel's operational capability and availability, and can significantly affect through-life maintenance costs. The development of reliable tools to assess a naval ship's fatigue life will enable better management of aging fleets and facilitate the design of more resilient hulls. Spectral fatigue analysis of ships involves applying hydrodynamic wave loads to a structural finite element model. The resulting stress response amplitude operators are combined with wave data to calculate stress spectra which are used with S-N curves to estimate the fatigue crack initiation life. In this paper, data from a naval vessel sea trial are used to validate STRUC_R, spectral fatigue analysis software developed by Cooperative Research Ships (CRS). The calculated stress spectra are compared with measurements at fifteen structural locations and found to be in reasonable agreement with several exceptions. The effect of using long-crested and two-dimensional seaway models of measured conditions are compared. Results closer to measurements are obtained with two-dimensional models, but long-crested results provide a reasonable approximation. As most available wave data are one-dimensional, this provides a better understanding of the uncertainty long-crested wave assumptions introduce in naval vessel stress spectra calculations.

1. INTRODUCTION

The rational design of ships to optimize scantlings and the use of higher strength steels have reduced the weight of hull structures. This can lead to higher cyclic stresses that may result in the development of fatigue cracks. Spectral fatigue analysis is a method to determine the fatigue crack initiation life for ship components under the assumption that dynamic wave loads are the main source of fatigue damage. Hydrodynamic wave loads are calculated for each combination of wave frequency, ship speed, and ship heading relative to the waves. These loads are applied to a finite element (FE) analysis model of a ship and the resulting stress transfer functions are calculated. The operational profile, the amount of time a ship is operated in given combinations of wave heights, wave periods, speeds, and headings relative to the waves are combined with the stress transfer functions to calculate the stress spectrum for each combination. The predictions made over long periods are calculated by a weighted sum of the short term damage. The sum is weighted by the proportion of time in each operational cell (speed, heading, load case, wave height, wave period). The cumulative damage is typically summed using the Palmgren-Miner law with Rayleigh statistics, which assume the response is narrow-banded. Further details of spectral fatigue analysis are provided by Chen and Mavrakis (1988).

Spectral fatigue analysis is used for marine structures due to the variability of waves. For example, it has been used to assess a hatch cover bearing pad in a Panamax container ship by Kukkanena and Mikkolab (2004), a connection of a main deck longitudinal to a transverse web

DRDC-RDDC-2015-P148

ISBN 978-88-940557-1-9

at the midship section of a dredging barge by Wang (2010), and hopper knuckles in a liquefied natural gas carrier by Park et al (2011). Guidelines for performing spectral fatigue analyses for ships and offshore structures are provided by Lloyd's Register (2014), Bureau Veritas (2008), and Det Norske Veritas (2014).
In this study, the results of a sea trial on a conventionally designed warship are compared with the root mean square (RMS) longitudinal stress and zero-crossing frequency (ω_z) calculated using spectral fatigue analysis software. The results were calculated using one-dimensional (1-d), or long-crested, and two-dimensional (2-d) wave spectrum models within the operational profile. The results from using these two seaway models are compared with measured data to provide a better understanding of the uncertainty that is introduced by using one-dimensional wave spectra, the data which are typically available.

2. METHODOLOGY

The analyses were performed using STRUC_R (see Thompson et al, 2013), spectral fatigue analysis software developed within Cooperative Research Ships (CRS). STRUC_R is a tool to map the hydrodynamic loads to an FE model, generate stress spectra, and calculate fatigue life estimates. The first step involves importing hydrodynamic and FE models, aligning them and adjusting their mass to ensure model compatibility. Afterwards, a wetted hull, the portion of the FE model exposed to water pressure, is created. Hydrodynamic forces (for each combination of speed, heading, and frequency) are imported and applied to the FE model nodes of the wetted hull. The FE files are exported to a solver and the FE results are imported from the solver and used to generate stress transfer functions for the finite element panels of interest. The operational profile (time in given sea condition, speed, and heading) is specified and combined with the stress transfer functions. This produces stress spectra and the resulting spectral moments for each combination of speed, heading, and wave spectrum. Although the STRUC_R analysis in this study was completed at this stage, typically it is used to generate fatigue life estimates and includes other functionality, including correcting fatigue estimates for mean stress effects and stress concentrations.
The hydrodynamic loads applied to the finite element model were determined using PRECAL_R, a linear three-dimensional frequency domain panel code also developed within CRS described by van Daalen and Sireta (2014). PRECAL_R is a potential flow code that can calculate motions as well as pressures on hull panels for each load case (combination of speed, heading, and frequency). The VAST FE solver (see Martec Limited, 2006), was used to calculate the displacements and stresses on the global FE model.
The displacements calculated in the global FE model were transferred to the local FE models using topdown analysis. For each load case, the displacements of global model nodes were transferred to coincident local master nodes sharing a common boundary. The remaining local model nodes sharing a common boundary with the global FE model were treated as slave nodes. The displacements of the slave nodes were defined in terms of the master nodes using linear interpolation.
The global FE model consisted of 71854 nodes and 156636 elements (primarily shell and beam elements) and is shown in figure 1. The 15 local models varied in size from approximately 4000 nodes and elements to 29000 nodes and 28000 elements. Typically, the local models extended to adjacent frames longitudinally and at least to the next longitudinal stiffener transversely. Stiffeners represented by beam and shell elements in the global models were refined using shell elements. An example of a local model is shown in figure 2. The hydrodynamic mesh was constructed using 11028 nodes and 10134 panels. The hydrodynamic model elements were approximately 15% greater than the FE model elements. Hydrodynamic calculations were made with PRECAL_R using the two nominal trial speeds (10 knots and 20 knots), 24 headings (15 degree increments), and 38 wave frequencies covering trial wave spectra (0.1 rad/s increments from 0.1 – 0.4 rad/s and 1.6 – 2.6 rad/s and 0.05 rad/s increments between 0.4 rad/s and 1.6 rad/s) for a total of 1824 different load cases.

ISBN 978-88-940557-1-9

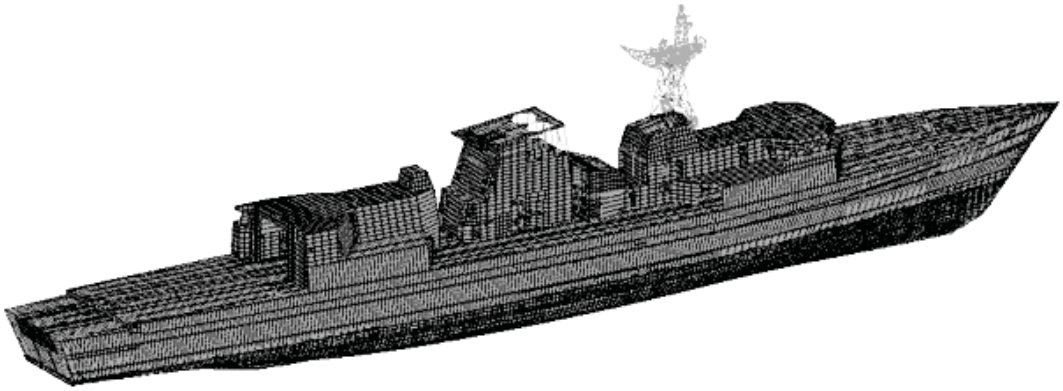

Figure 1. Finite element model of analyzed naval ship.

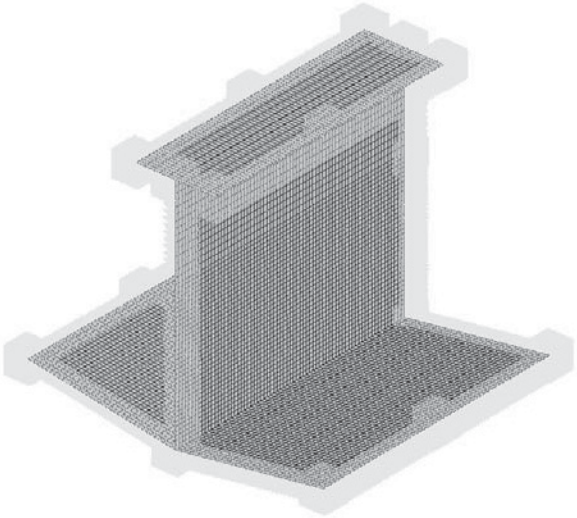

Figure 2. Local model containing area of Gauge s26 on web of keel girder. The large shaded cubes along the perimeter are master nodes, the rest of the shading shows the slave node locations.

The measured sea conditions were represented in the operational profile in the analysis using measured 2-d wave spectra and two-parameter Pierson-Moskowitz spectra (long-crested), as outlined by Stansberg et al (2002), with significant wave height and peak period determined from the measured data. The measured 2-d wave spectra account for waves coming from all directions over all measured frequencies, while the two-parameter Pierson-Moskowitz spectrum is a uni-directional simplification. The 2-d wave spectra are more accurate, but require spectral energy density values for each combination of heading and frequency, in this case, 123 frequencies between 0 and 3.8 rad/s and 121 headings over 360 degrees. Examples of each of the spectrum types (2-d spectral density integrated over all headings) from one of the trial runs are shown in figure 3. The differences shown in the example spectra are typical from this trial: the peak energy density of the 2-d spectrum tends to be higher while the long-crested spectrum is smoother, as would be expected of a spectrum based on a mathematical model. Although the peak of the 2-d spectrum shown in figure 3 is much higher, the value of the integral of the 1-d spectrum is only 8% lower.

ISBN 978-88-940557-1-9

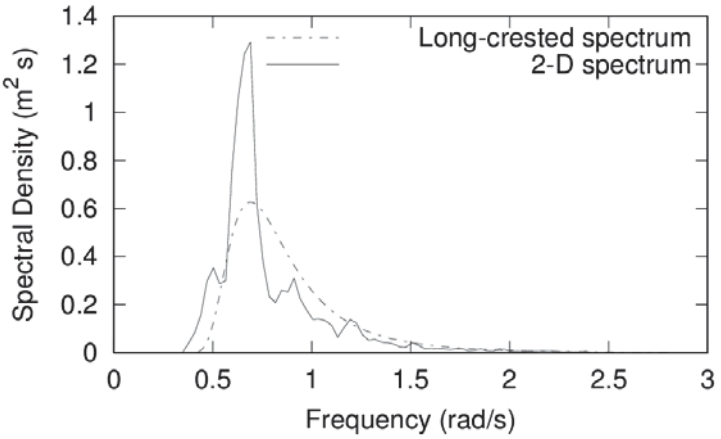

Figure 3. Example 2-d and long-crested wave spectra from a single trial run.

The ship trial considered in this study began on the Grand Banks off Newfoundland, Canada, moved south of the Avalon Peninsula, and finished east of Sable Island. It consisted of 75 trial runs of 20 to 30 minutes. During each run, the speed (nominally 10 or 20 knots) and heading were held constant. Trial runs were made with a variety of headings into the waves in seaways with significant wave heights of 0.7 m – 6.1 m. Wave data was measured by a freely floating Triaxys wave buoy. Fifteen uniaxial strain gauges were applied longitudinally at several cross sections on main deck girders, side-shell longitudinals, and on the keel structure. The gauges were located at 3 longitudinal sections, approximately 20, 50, and 65 percent of the length between perpendiculars from the forward perpendicular. Strain measurements were sampled at 50 Hz and filtered using low-pass anti-aliasing filters set at 20 Hz cutoff. The strain measurements were converted to the frequency domain, contributions due to whipping were filtered out, and RMS strain and zero-up-crossing frequency were calculated. All gauges were installed on the web of the local structure near the adjacent shell or deck plating. Details about the gauge locations are shown in table 1 below. The stresses were derived with Hooke's Law as uniaxial gauges were used.

Table 1. Strain gauge locations

Gauge Number	Approximate longitudinal position [% of L_{pp} from bow]	Gauge Location. Gauges located on web of component near plating
S15	20	Top of centerline longitudinal bulkhead under #4 deck
S17	20	Side shell longitudinal 20 - port
S18	20	Side shell longitudinal 20 - starboard
S19	20	Main deck girder - port
S20	20	Main deck girder - starboard
S26	50	Bottom of keel girder
S27	50	Side shell longitudinal 20 - port
S28	50	Side shell longitudinal 20 - starboard
S29	50	Longitudinal bulkhead – mid-way between centreline and side shell - port
S30	50	Longitudinal bulkhead – between centreline and side shell – starboard
S33	65	Side shell longitudinal 8 - port
S34	65	Side shell longitudinal 20 - Port
S35	65	Longitudinal 20 - Starboard
S36	65	Main Deck Girder - Port
S37	65	Longitudinal bulkhead – between centreline and side shell – starboard

ISBN 978-88-940557-1-9

The RMS stress and zero-up-crossing frequency measured during the sea trial were compared to the calculated values using a Matlab script to perform linear regression and calculate statistical values.

3. RESULTS

The two seaway models were compared to identify discrepancies. The zeroth and second spectral moments were used to quantify the models for each trial run. The spectral moments M_n of general order n, as outlined by DNV (2010), are defined as:

$$M_n = \int_0^\infty \omega^n S(\omega)\, d\omega \tag{1}$$

where ω is the angular frequency, $S(\omega)$ is the wave spectrum, and n = 0, 1, 2, …The significant wave height and zero-up-crossing frequency can be estimated by $4\sqrt{M_0}$ and $2\pi\sqrt{M_2/M_0}$, respectively. The zeroth spectral moments, M_0, of the long-crested spectra were, on average, 6% lower than those of the 2-d spectra. The standard deviation of the ratio of 1-d to 2-d M_0 values was 0.04. In 4 of the 75 trial runs M_0 for the 1-d spectrum was more than 12% lower than M_o for the 2-d spectrum. The four trial runs where the agreement was poorer had the lowest significant wave heights and wave energy was measured over a broader frequency range in the 2-d spectra than in the other trial run wave spectra. The M_2 values for the 1-d spectra were 2% greater, on average, than the value for the 2-d spectra and the standard deviation of the ratio was 0.19. The range of the ratio was from 0.5 to 1.5.
The stress spectrum for each trial run was generated by multiplying the trial run wave spectrum and the square of the stress transfer functions for the element considered. The RMS stress and the zero-up-crossing frequency can be estimated by $\sqrt{M_0}$ and $\sqrt{M_2/M_0}$, respectively. Several statistics were used to compare the measured and calculated results. Linear regression through the origin was used with the STRUC_R results as the dependent variable and strain gauge measurements as the independent variable. As the regression was through the origin, the coefficient of determination (R^2) was determined (see Eisenhauer, 2003) as:

$$R^2 = \frac{\sum(fitted\ value)^2}{\sum(STRUC\_R\ value)^2}. \tag{2}$$

The mean of the ratio of the calculated result to the measured result was also calculated for each gauge, as was the coefficient of variation of root-mean-square deviation (CV(RMSD)), which is defined in equation 3.

$$CV(RMSD) = \frac{\sqrt{\frac{\sum_{i=1}^{\#\ trial\ runs}(Calculated - Measured)^2}{\#\ trial\ runs}}}{Mean\ of\ measured\ parameter} \tag{3}$$

Comparisons of the calculated results to measured data are shown in the tables below. Table 2 shows the RMS stress results and table 3 shows the ω_z results.

ISBN 978-88-940557-1-9

Table 2. Comparison of measured and calculated RMS stress values for all trial runs.

Gauge Number	Regression Slope (STRUC RMS / Gauge RMS)		R^2		CV(RMSD)		Mean of STRUC RMS/ Gauge RMS	
	1-d	2-d	1-d	2-d	1-d	2-d	1-d	2-d
S15	1.39	1.31	0.91	0.98	0.68	0.42	1.47	1.42
S17	1.16	1.20	0.67	0.80	0.87	0.67	1.36	1.47
S18	1.31	1.63	0.30	0.54	2.20	1.79	1.47	2.02
S19	1.03	1.10	0.54	0.64	1.16	1.03	1.41	1.64
S20	1.13	1.15	0.55	0.67	1.23	0.99	1.59	1.72
S26	1.05	0.98	0.91	0.99	0.39	0.13	1.25	1.05
S27	2.36	3.09	0.33	0.63	3.95	3.42	2.33	3.17
S28	2.32	3.01	0.33	0.63	3.84	3.32	2.27	3.11
S29	0.98	0.92	0.91	0.98	0.37	0.17	1.16	1.02
S30	1.04	0.97	0.91	0.99	0.39	0.13	1.21	1.03
S33	1.37	1.31	0.81	0.90	0.89	0.64	1.70	1.61
S34	1.93	2.48	0.32	0.61	3.19	2.71	2.02	2.70
S35	1.98	2.53	0.34	0.61	3.21	2.73	2.00	2.72
S36	2.19	2.08	0.83	0.91	1.81	1.48	2.71	2.58
S37	1.36	1.29	0.84	0.92	0.81	0.56	1.67	1.56

Table 3. Comparison of measured and calculated ω_z values for all trial runs using long-crested waves.

Gauge Number	Regression Slope (STRUC ω_z / Gauge ω_z)		R^2		CV(RMSD)		Mean of STRUC ω_z / Gauge ω_z	
	1-d	2-d	1-d	2-d	1-d	2-d	1-d	2-d
S15	0.77	0.90	0.90	0.99	0.37	0.15	0.84	0.92
S17	0.86	0.74	0.90	0.98	0.33	0.29	0.86	0.75
S18	0.79	0.86	0.90	0.94	0.36	0.28	0.76	0.80
S19	0.65	0.84	0.92	0.99	0.43	0.20	0.69	0.85
S20	0.68	0.81	0.91	0.98	0.42	0.24	0.73	0.85
S26	0.83	0.94	0.91	1.00	0.33	0.10	0.85	0.95
S27	0.75	0.75	0.90	0.96	0.37	0.30	0.74	0.74
S28	0.76	0.76	0.90	0.96	0.36	0.30	0.75	0.75
S29	0.83	0.95	0.91	1.00	0.33	0.09	0.85	0.94
S30	0.86	0.95	0.92	0.99	0.31	0.09	0.87	0.96
S33	0.78	0.93	0.92	0.99	0.34	0.14	0.81	0.92
S34	0.74	0.76	0.90	0.96	0.38	0.30	0.75	0.75
S35	0.73	0.76	0.91	0.96	0.37	0.30	0.72	0.75
S36	0.80	0.93	0.92	0.99	0.32	0.12	0.81	0.91
S37	0.79	0.93	0.92	0.99	0.34	0.13	0.82	0.92

4. DISCUSSION

The results in table 2 show reasonably good agreement between the calculated RMS stress and trial data. In terms of agreement and scatter, the results fit into three groups: the side-shell longitudinal gauges located about 0.3 m above the waterline (s17, s18, s27, s28, s34, s35), s36

ISBN 978-88-940557-1-9

on the web of the main deck girder, and the rest of the gauges. Examples of the first group (s28) and the third group (s15) are shown in figure 4.

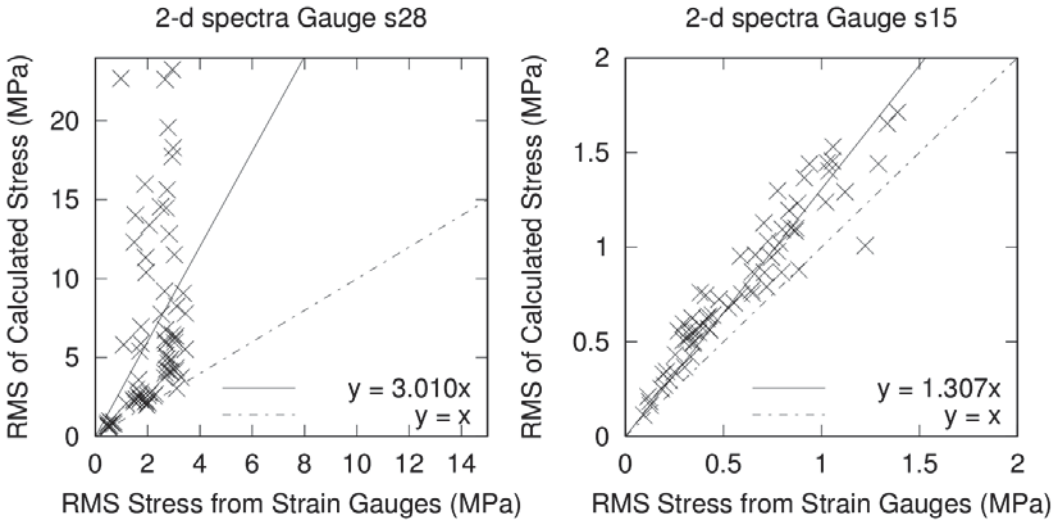

Figure 4. Examples of calculated RMS stress vs RMS stress derived from strain gauge

measurements. Linear regression and perfect correlation lines also shown.

The gauges in the first group exhibit consistent over-prediction of stress and a great deal of scatter, with the gauges near the bow (s17 and s18) giving better results than those near mid-ship. The results from gauge s17 may be somewhat misleading because measured results were only available for 23 of the 75 trial runs, possibly omitting some of the runs that produced outliers in the other gauges in this group. The five gauges in this group (omitting s17) had the highest CV(RMSD) values, indicating the poorest agreement. These gauges were above the waterline and would have been exposed to intermittent wetting. The hydrodynamic analysis assumes a constant waterline, so this could cause a discrepancy. The calculated RMS stress results for gauge s36 are approximately double the measured values, but there is less scatter than observed in the first group of gauges. The global FE model contains an opening adjacent to the main deck girder where s36 was applied. This area is shown on the ship drawings as containing portable plate, but no indications of the portable plate were found on a recent visit to the ship. The opening in the FE model could act as a stress concentration that may not be present, or may not be as significant as modeled, on the actual ship.

The rest of the gauges show good agreement between calculated and measured RMS stress values. The regression line slopes and the mean ratios of calculated results to measurements are generally greater than unity, indicating calculated values are usually over-predictions.

The agreement between calculated values of ω_z and those derived from strain gauge measurements (table 3) was good and there was far less scatter than was observed in the RMS stress comparisons. The slope of the regression lines varied from 0.65 – 0.86 for the long-crested waves and 0.74 – 0.95 for the 2-d waves. However, the calculated values under-predicted values derived from measurements as all values of the regression line slope and the mean of the ratio of calculated to measured values were less than unity. This is consistent with over-prediction of RMS stress, as the RMS stress is proportional to the square root of the zeroth spectral moment, and ω_z is the square root of the second spectral moment divided by the zeroth spectral moment. Examples of the ω_z results are shown in figure 5 for Gauge s20 (web of main deck girder) and Gauge s35 (side-shell longitudinal near waterline).

ISBN 978-88-940557-1-9

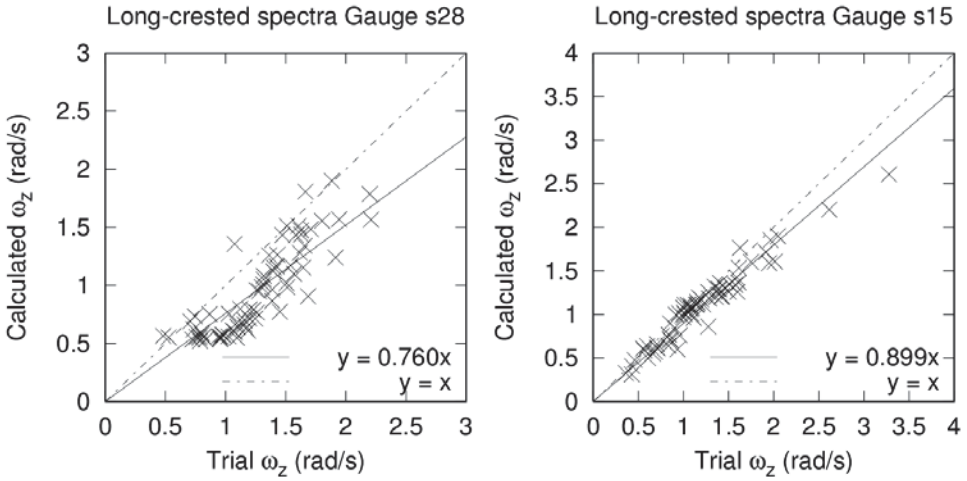

Figure 5. Examples of calculated versus trial zero-up-crossing frequency. Linear regression and perfect correlation lines also shown.

Generally, the results obtained using the 2-d wave spectra and long-crested wave spectra are similar. The CV(RMSD) values were at least 10% lower for both RMS stress and ω_z for all of the gauges when using the 2-d spectra. This is as expected: a better characterization of the sea state provided more accurate results.

The slopes of regression lines changed between the two types of spectra, but the 2-d results were not consistently better for the RMS stress. The mean values of the ratio of calculated to measured RMS stress data were closer to unity when using the 2-d spectra except for gauges s19 and s20 which were similar and the side-shell longitudinal stiffeners which were significantly worse. However, for comparison of the ω_z results, the regression slopes and means of the calculated to measurement ratios were better for all gauges when using 2-d wave spectra.

There was more scatter in the long-crested wave results. The R^2 values were higher when using 2-d wave spectra and there were fewer outliers. Analyses with long-crested wave spectra produced 18 values of RMS stress (out of 1045 calculations) that were 10 times greater than the values derived from measurements and 11 less than 0.2 times values derived from measurements. The use of 2-d wave spectra reduced this to 9 values greater than 10 times measurements and none less than 0.2 times measurements.

Many of the same conclusions can be drawn from the use of long-crested wave spectra and 2-d wave spectra. Both sets of results show reasonable agreement of RMS stress and ω_z between calculations and measurements. For s18, however, the 2-d spectra indicate that calculated values are questionable while the 1-d spectra suggest they are reasonable. The 2-d results of s18 are consistent with calculated results of other side-shell longitudinal stiffeners near the waterline. Measured ω_z values generally agree with 2-d wave spectra ω_z results better than the 1-d spectra ω_z. After analyzing the results, the ship motions from PRECAL_R were reviewed and excessive motions in surge, sway, yaw, and roll were noted within 30° of following seas. This is consistent with outliers within 30° of following seas that produced significant over-predictions. This is believed to be due to the low encounter frequencies near following seas which could lead to a singularity in the hydrodynamic analysis.

Analysis of this type involves uncertainty in a number of the parameters. There are uncertainties in the FE model of the ship introduced by the variations in material properties and geometry, discretization of the ship into finite elements, use of shell elements, and uncertainties in the mass distribution. The characterization of the seaway will have uncertainties whether a mathematical model or seaway measurements are used. There will also be uncertainties in the measurement of ship speed and heading, strain, and wave height. Of course, linear assumptions in the hydrodynamic loading will introduce error. Whipping, intermittent wetting, and other non-linear processes will increase the uncertainty in the stress spectra. In this study, there are overly large ship motions in following seas as well as a problem with the analysis of the side-shell longitudinal stiffeners near the waterline that appear to be contributing to the variation between measured and calculated results.

ISBN 978-88-940557-1-9

5. CONCLUSIONS

In this study, calculated stress spectra parameters were compared with trial data for a conventionally-designed warship using spectral fatigue analysis. Analyses were conducted using both 1-d and 2-d wave spectra for comparison. The calculated values of RMS stress and ω_z are in reasonable agreement with values derived from strain gauge measurements, although there are significant over-predictions of RMS stress in the area of a potential error in the global FE model and in side-shell longitudinal stiffeners approximately 0.3 m above the waterline. The zero-up-crossing frequencies are in good agreement and there is less scatter in their values, but the calculated values are consistently lower than those derived from measurements.

The results from the 2-d wave spectra are generally in better agreement with trial data than results from analyses with long-crested wave spectra; the coefficient of variation of root-mean-square deviation values decreased by at least 10% when using 2-d spectra over long-crested spectra. However, similar conclusions can be drawn using either set of wave spectra. Generally, the use of long-crested wave spectra in this study tended to over-predict RMS stress and under-predict zero-up-crossing frequency. Although the use of 2-d wave spectra reduces the uncertainty in spectral fatigue analysis, it did not appear to be the most substantial factor in this analysis. This is reassuring, as 2-d wave spectra are typically unavailable for spectral fatigue analysis; wave statistics typically provide significant wave height and peak period and may contain information on the distribution of wave directions.

Future work is necessary to compare the use of 1-d and 2-d wave spectra on fatigue initiation predictions. Higher RMS stress values will reduce the predicted fatigue life while lower ω_z values will reduce the number of stress cycles and increase the fatigue life. Improvements to the excessive ship motions calculated near following seas and improvements to calculations of the side-shell longitudinal stiffeners near the waterline will also be sought in the future.

ACKNOWLEDGEMENTS

Thanks to many members of the Warship Performance section at DRDC Atlantic Research Centre for their assistance, especially James Nickerson, for his work improving the STRUC_R software.

REFERENCES

Bureau Veritas (2008) “Spectral Fatigue Analysis Methodology for Ships and Offshore Units”, Guidance Note NI 539 DT R00 E, July 2008.

Chen, Y. N., Mavrakis, S.A. (1988) “Closed-form Spectral Fatigue Analysis for Compliant Offshore Structures” Journal of Ship Research, 1988, Vol. 32, pp. 297 – 304.

Det Norske Veritas (2010) “Environmental Conditions and Environmental Loads”, Recommended Practice DNV-RP-C205, October 2010.

Det Norske Veritas (2014) “Fatigue Assessment of Ship Structures”, Classification Note 30.7, April 2014.

Eisenhauer, J.G. (2003) “Regression through the Origin”, Teaching Statistics, Vol. 25, No. 3, 2003.

Kukkanena, T., Mikkolab, T.P. (2004) “Fatigue Assessment by Spectral Approach for the ISSC Comparative Study of the Hatch Cover Bearing Pad”, Marine Structures, Vol. 17, pp.75 – 90.

Lloyd’s Register (2014) “ShipRight Design and Construction, Fatigue Design Assessment - Application and Notations”, September 2014”.

Martec Limited (2006) “Vibration and Strength Analsysis Program (VAST) Version 9.0 User’s Manual”.

Park, T., Jang, C., Suh, Y., Kim, B. (2011) “A Parametric Study Based on Spectral Fatigue Analysis for 170k LNGC” International Journal of Naval Architecture and Ocean Engineering, Vol. 3, pp. 116 – 121.

Stansberg, C. et al (2002) “The Specialist Committee on Waves Final Report and Recommendations to the 23rd ITTC”, Proceedings of the 23rd ITTC – Volume II, pp. 505 – 736.

Thompson, I., Stredulinsky, D., Gannon, L., Oakey, S. (2013) “STRUC_R v. 2.4 User’s Manual”, ECR 2013-026, October 2013.

van Daalen, E.F.G, Sireta, F-X. (2014) “PRECAL_R User Manual, Version 1.0.0”, Report No.: 21447-6-RD, June 2014.

Wang, Y. (2010) “Spectral Fatigue Analysis of a Ship Structural Detail – A Practical Case Study”, International Journal of Fatigue, Volume 32, pp.310-317.

ISBN 978-88-940557-1-9